ISOPROPYL ALCOHOL DECOMPOSITION OVER MOLYBDENA-ALUMINA CATALYST

K.T. Seo, S.C. Kang, H.J. Kim, S.K. Moon*

Department of Chem. Engineering, Hanyang University, Seoul, 133, Korea.

(Received 13 May 1985• accepted 25 July 1985)

Abstract— The decomposition of isopropyl alcohol was chosen as a probe reaction of acid-base property of molybdena-alumina catalyst. The catalytic kinetics was examined on the oxidized catalyst. The kinetics of the dehydration (yielding propene) and the dehydrogenation (yielding acetone) obeyed the Langmuir-Hinshelwood mechanism in which the rate determining step is the desorption of water for the former and the sur face reaction for the latter, respectively. The effect of varying the extent of reduction of the catalyst was also studied. The trend of variation with the reduction was fairly consistent with the surface chemistry of the catalyst.

1. INTRODUCTION

There is still confusion surrounding the nature of the catalyst based molybdenum oxide supported on alumina [1]. Interest in these catalysts stems from their hydrodesulfurization of organic feed stocks and from their promotion of other reactions such as the hydrogenation and the metathesis of olefins. In order to develop more active and selective catalysts it is necessary to determine the structure of the catalysts and understand the properties of these catalysts that produce their catalytic activity and selectivity. One of such properties is acid-base property of catalyst .Although much attention has been paid to the role of acidity, its base property may also be a significant factor. To investigate the strength, amount and structure of acid and base site, one can utilize various methods of acid-base property measurements such as titration, calorimetry and infrared spectroscopy. But the restriction which has been encountered concerns the size of probe molecules as well as its strength. Frequently, to obtain the information of acid-base property of catalyst, the probe reaction is considered to be a more potential method than characterization studies because the former measures catalytic properties, upon which a catalyst is selected for use for a reaction.

Recently, the activity for the dehydration of isopropyl alcohol or the isomerization of butene in the presence of an excess of air is reported to be a good measure of acidity of metal oxide catalysts [2-7]. Fairly good correlations are found between the acidity measured by adsorption of ammontia or pyridine and the activity for dehydration of isopropyl alcohol (IPA) and isomerization of 1-butene [4]: the catalytic activity for dehydration of IPA to propene (r_p) is proportional to the acidity of a catalyst.

$$r_p = k_p \cdot \text{acidity} \quad (1)$$

Support of this kinetics model has been found in many mechanistic studies [8,9], which have determined that acid sites are important in the reaction. On the other hand, the activity for dehydrogenation of IPA to acetone (r_k)is assumed to be proportional to the acidity and basicity of catalyst, because the dehydrogenation is considered to proceed by a concerted mechanism [3,5,6]:

$$r_k = k_k \cdot \text{acidity} \cdot \text{basicity} \quad (2)$$

The concentration of basic sites was found by measuring the rate of the dehydration reaction along with that of the dehydrogenation and combining eq. (1) and (2):

$$\text{basicity} = \frac{k_k\, r_k}{k_p\, r_p} = k' \frac{r_k}{r_p} \quad (3)$$

In fact, a good correlation is found between r_k/r_p and the amount of carbon dioxide irreversibly adsorbed [4, 6]. Thus, r_k/r_p can be used as a measure of catalyst basicity.

The above concept is expected to be useful in so far to study the acid-base properties of molybdena-alumina catalyst.

With the aim of obtaining information on the acid-base properties for molybdena-alumina, the kinetics of the IPA decomposition on the unreduced catalyst was studied and the dependence of acid-base property upon reduction of catalyst also studied.

*To whom correspondence should be addressed.

2. EXPERIMENTAL

Catalyst preparation and characterization

Molybdena-alumina catalyst (Mo-Al_2O_3) was prepared by the equilibrium adsorption medthod [10]. This was made by placing a 80 grams of η-Al_2O_3 (Davison high surface area alumina SMR-7-5691, 30/60 mesh) in contact with 20 liters of 0.01 M solution of ammonium para-molybdate (Matheson, Coleman and Bell AX 1310) for 100 hours, followed by filtering and drying at 380 K before a final air calcination at 773 K for 15 hours. Initial pH of solution was adjusted to 5.1 using HNO_3 and/or $(NH_4)OH$. Specific surface area of the catalyst, determined by the BET, was 200 m^2/g. The catalyst was analyzed by GALBRAITH Lab. Inc., Tennessee, U.S.A. The content of molybdenum in the catalyst was 7.6%.

Catalyst treatment

The catalyst was subjected to several treatments in order to alter system matically its surface characteristics. A raw catalyst was placed in a quartz microreactor and subjected to an overnight pretreatment at 773 K in flowing dry oxygen (50ml/min). It was then evacuated for 1 hour at the temperature of reduction. They were used either directly in this state or after reduction with hydrogen. The reduction were performed at 673 K using mixtures of helium and hydrogen. The total flow rate of gases was 50ml/min. The individual flow rates of the two gases were adjusted to give different hydrogen partial pressures. The conditions used are shown in Table 1.

Gases

All gases were obtained from commercial sources. The helium used as carrying gas and/or diluent gas was further purified by passage through pyrex traps containing reduced copper turnings maintained at 520 K and then through molecular sieve 13X trap cooled by liquid nitrogen. Hydrogen as reduction agent was purified by commercial Deoxo unit (Engelhard), followed by a molecular sieve 13X trap held at 78 K and oxygen, by only molecular sieve 13X trap at room temperature.

Apparatus and procedures

The decomposition of IPA was carried out using a microcatalytic continuous reaction system as shown in Fig. 1. The catalyst was supported on a quartz fritted disk in a quartz reactor which was connected to the reaction system. The reactor is in an electrically heated and regulated to within about 1 K. The introduction of a thermocouple close to the catalyst allows to measure the reaction temperature. The IPA fed into a helium carrying gas stream by a syringe pump (Sage Instrument model 341A) was carried over the catalyst at 1 atm of total pressure. Changing the flow rate of IPA by syringe pump, the pressure of IPA is modified. At the outlet of the reactor, gas samples were taken to the chromatographic apparatus (Shimadzu GC 4C-PT), which uses a column of polyethylene glycol 1500 (15%, 3m) that seperates propene, di-isopropyl ether, acetone, IPA and water. Chromatographic condition: carrier gas, helium; column pressure, 0.25Kg/cm^2; column temperature, 370K; detector, thermal conductivity.

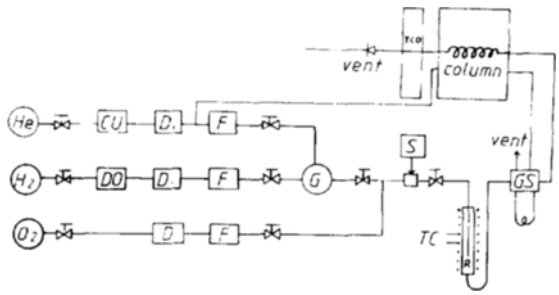

Fig. 1. Schmatic diagram of the experimental apparatus. The notation is as follows: CU, copper trap (520K); D, molecular sieve 13 X; D_1, molecular sieve 13X liquid nitrogen trap; DO, deoxo purifier; F, flow meter; G, gas mixer; GS, gas sampler; R, reactor; S, syringe pump; TC, temperature controller.

Table 1. Conditions for the catalyst treatments.

Catalyst symbol	Oxidation			Reduction			
	Temperature (K)	Time (hr)	Oxygen flow rate (ml/min)	Temperature (K)	Time (min)	Hydrogen flow rate (ml/min)	Helium flow rate (ml/min)
Mo-Al_2O_3(0)	770	10	50	–	–	–	–
Mo-Al_2O_3(1)	770	10	50	670	5	9	41
Mo-Al_2O_3(2)	770	10	50	670	60	9	41
Mo-Al_2O_3(3)	770	10	50	670	360	12	38

3. RESULTS

Kinetics of IPA decomposition over a oxidized Mo-Al_2O_3

In the absence of catalyst, no reaction occured in the temperature range explored. The experimental data reported below which mostly refer to the temperature range, 450 to 510 K, have therefore been obtained at temperatures well below the region where homogeneous decomposition or reactor-wall reactions occur.

For the first 3 hours on the time-on stream, the conversion of IPA decreased sharply and maintained at constant value of conversion thereafter. Unless otherwise indicated, conversion quoted in the following sections refer to these constant value. No isopropyl ether was detected as a reaction product in the temperature range explored.

One of the first observations of this study was that the catalysts are more active for the dehydration, yielding propylene than for the dehydrogenation, yielding acetone. We present below the individual results for dehydration and dehydrogenation. Throughout the whole paper, we employ the following subscripts: A = IPA, P = propene, W = water, K = Acetone and H = hydrogen.

a) Dehydration

In order to discriminate the model of Langmuir-Hinshelwood (L-H) type equations, the intrinsic parameter method proposed by Yang and Hougen was used [11, 12]. Fig. 2 shows the conversion to propene (x_p) versus space time (W/F_A°) diagram, from which the initial rates were obtained by numerically differentiating the data at $W/F_A^\circ = 0$. The initial rates were independent upon the initial IPA pressure. This clearly shows that the desorption of product is the rate-determining step [12]. On this premise, let's consider the sequence of steps listed below.

1. Ausorption of IPA.
2. Surface reaction involving the release of propylene, water remaining adsorbed.
3. Desorption of water.

The desorption of water to be rate-controlling is presumed to be slower than the adsorption and surface reaction steps. A L-H type rate equation consistent with this mechanism can be derived. This equation for IPA dehydration

$$A \rightleftharpoons P + W \tag{4}$$

follows:

$$r_P = \frac{k\,K\left(\frac{P_A}{P_P} - \frac{P_W}{K}\right)}{1 + K_A P_A + K\,K_W \frac{P_A}{P_P}} \tag{5}$$

From eq. (5), the initial rate expression is obtained as follows,

$$r_P^\circ = \frac{k\,K\,P_A^\circ}{K\,K_W\,P_A^\circ} = \frac{k}{K_W} \tag{6}$$

which leads to calculation of the value of k/K_W at various temperatures. In order to determine all the constants from the eq. (5), it is rearranged into

$$\left(\frac{r_P^\circ}{r_P} - 1\right)\frac{K\,P_A}{P_P} - \frac{r_P^\circ}{r_P}P_W = \frac{1}{K_W} + \frac{K_A}{K_W}P_A \tag{7}$$

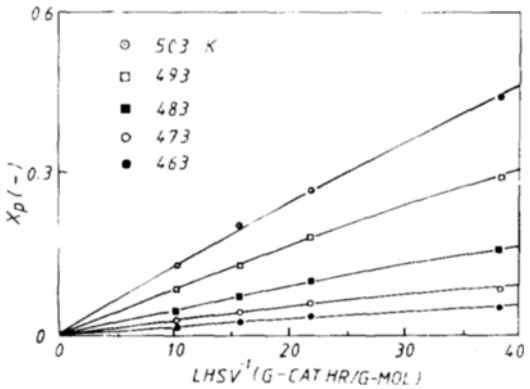

Fig. 2. IPA dehydration. Conversion to propene (x_p) versus space time at various temperatures.

Table 2. Values of the kinetic parameters calculated at various temperature.

Temperature (K)	Dehydration				Dehydrogenation	
	$K^* \times 10^{-4}$	$k \times 10^7$	K_A	$K_W \times 10^4$	$k_{sr} \times 10^4$	K'_A
463	3.49	0.7	168	3.6	3.8	8.3
473	4.53	1.0	125	3.0	5.1	7.5
483	5.83	1.7	90	2.8	6.8	7.2
493	7.42	3.1	67	2.6	9.2	6.9
503	9.34	4.7	57	2.7	11.8	6.8

* Calculated from free energy of formation data.

From which, the parameters k, K_W and K_A can be estimated by linear regression (Table 2). The overall equilibrium constant K was calculated from free energy of formation data. Arrhenius plots for parameters are shown in Fig. 3.

b) Dehydrogenation

Kinetic data of dehydrogenation of IPA, yielding acetone, are of the shape shown in Fig. 4. Exprimental dependences of acetone-formation rate r_k on partial pressures of IPA in the feed p_A^o were fitted by means of linear regression to possible five L-H type rate equations. The best rate equation was selected using the criterion of maximal likelihood; the following rate equation gave very good fit.

$$r_k = \frac{k_{sr} K'_A P_A^o}{(1+K'_A P_A^o)^2} \qquad (8)$$

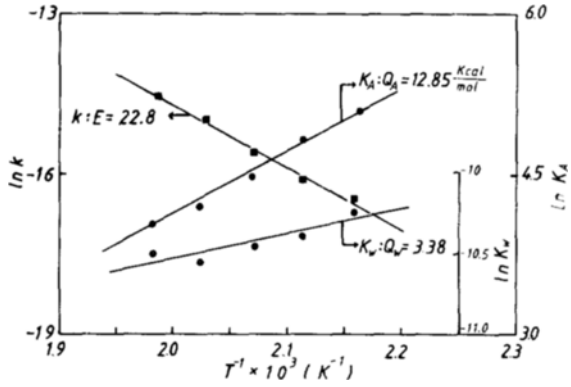

Fig. 3. Dependence of kinetic parameters in eq (5) on temperature.

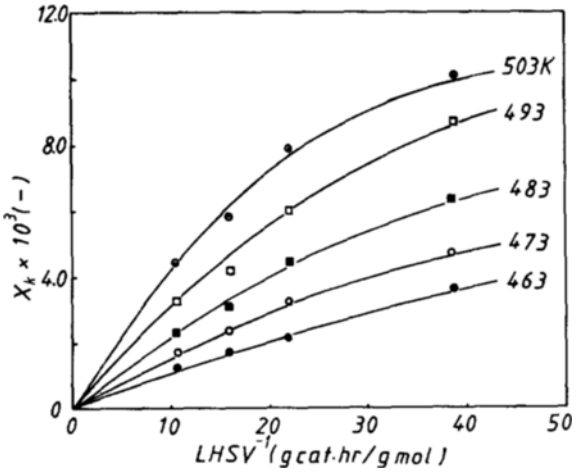

Fig. 4. IPA dehydrogenation. Conversion to acetone (x_k) versus space time at various temperatures.

In terms of the L-H mechanism, eq. (8) corresponds to surface reaction on dual sites as the rate-determining step and to negligible product adsorption. This equation was also established based on the assumption that the dehydrogenation takes place on the sites different from those for the dehydration.

To determine the parameters, eq. (8) is linearized into

$$\sqrt{\frac{P_A^o}{r_k}} = \frac{1}{\sqrt{k_{sr} K'_A}} + \frac{K'_A}{\sqrt{k_{sr} K'_A}} P_A^o \qquad (9)$$

which leads to the plot shown in Fig. 5 and estimate the parameters k_{sr} and K_A'. Fig. 6 shows the good consistency between the experimental data and the calculated values. The estimated parameters are listed in Table 2.

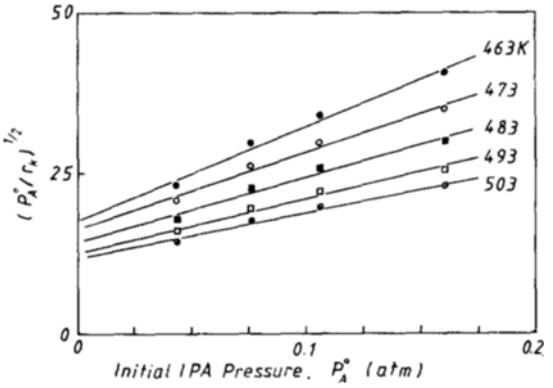

Fig. 5. Relationship between $(P_A^o/r_k)^{\frac{1}{2}}$ and P_A^o

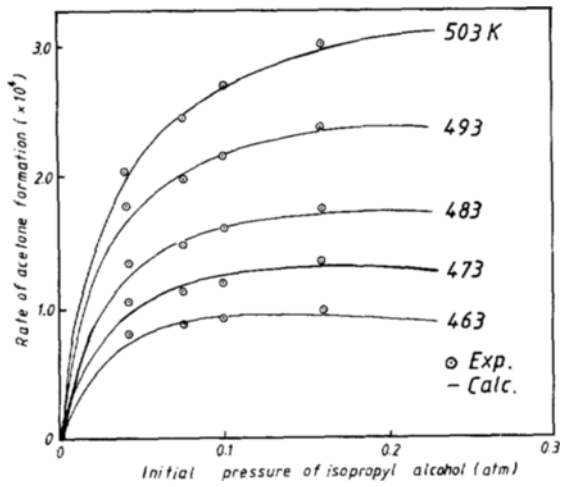

Fig. 6. Comparision between experimental and theoretical reaction rate of IPA to acetone.

Arrhenius plots for k_A' have the shape shown in Fig. 7.

Dependence of acid-base property on reduction

The Mo-Al_2O_3 catalyst was subjected to several treatments to alter the surface characteristics; in particular, acid-base property. The catalysts were designated as Mo-Al_2O_3(n) with the treatment conditions. The number, n, in parenthesis represents the treatment condition as indicated in Table 1. The effect of reduction on the decomposition of IPA at 503 K are of the shape shown in Fig. 8 and 9, respectively. The variation of propene-formation rate due to the reduction condition is represented in Table 3, which shows the acidity variations [2-7]. One of the interesting observations is the rapid decay of r_p for the slightly reduced catalyst, Mo-Al_2O_3 (1).

From the data in Table 3, it is easy to find the variation of r_k/r_p as a rough measure of basicity on the catalyst due to the reduction.

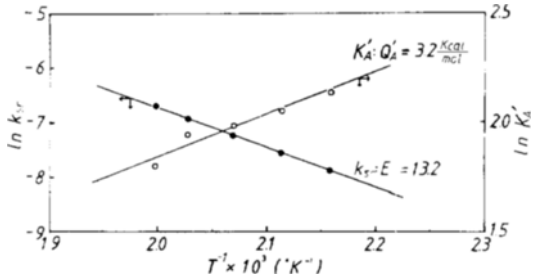

Fig. 7. Dependence of kinetic parameters in eq. (8) on temperature.

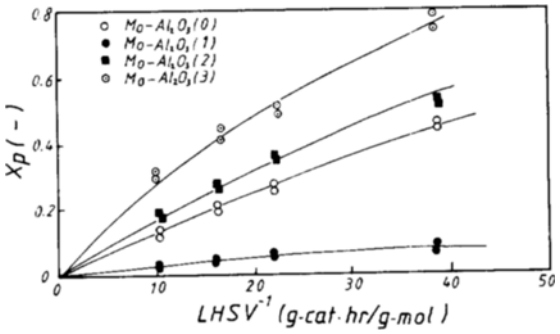

Fig. 8. Dependence of conversion to propene on the catalyst treatment; reaction temperature = 503K.

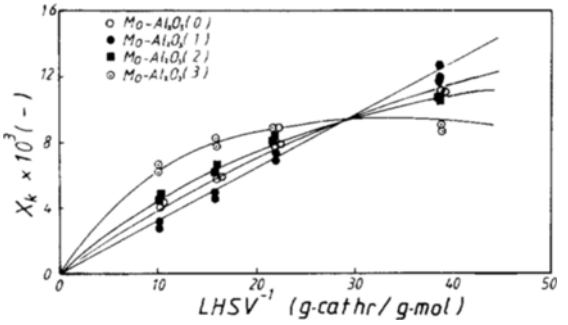

Fig. 9. Dependence of conversion to acetone on the catalyst treatment; reaction temperature = 503K.

4. DISCUSSIONS

Kinetics of IPA decomposition on a oxidized Mo-Al_2O_3

In this study, Mo-Al_2O_3 catalysts are proposed to be probed by the alcohol decomposition reaction. The decompostion of IPA to propene and water (dehydration, eq. 10) or to acetone and hydrogen (dehydrogenation, eq. 11) are common probe reactions that are used

Table 3. Variation of acidity and basicity with treatments of the catalyst.

Catalyst treatment	This work		Suarez's data (24)**	
	$r_p \times 10^3$ (g-mol/g-cat hr)	$r_k/r_p \times 10^2$ (-)	Pyridine molecules adsorbed/$m^2 \times 10^{-18}$ $B_{py}+L_{py}(I)+L_{py}(II)$*	$L_{py}(I)$
Oxidized	11.92	2.54	1.150	0.710
Reduced 5 minutes	2.20	14.16	1.240	0.671
Reduced 1 hour	14.50	2.07	1.273	0.897
Reduced 6 hours	20.98	1.25	1.150	1.016

* These IR data were obtained after evacuation at 370K. B_{py} represents the amount of pyridine adsorbed on Bronsted acid sites; $L_{py}(I)$, on the weaker type of Lewis acid site and $L_{py}(II)$, on the strong type of Lewis acid site.

** The catalyst used was reduced in a static circulation system.

with catalysts that have acid and base functions [7]:

$$CH_3CHCH_3 \rightarrow CH_3CH=CH_2+H_2O \quad (10)$$

$$CH_3\overset{OH}{\overset{|}{C}}HCH_3 \rightarrow CH_3\overset{O}{\overset{\|}{C}}CH_3+H_2 \quad (11)$$

Propene formation tends to be approximately zero order reaction with respect to IPA concentration. We

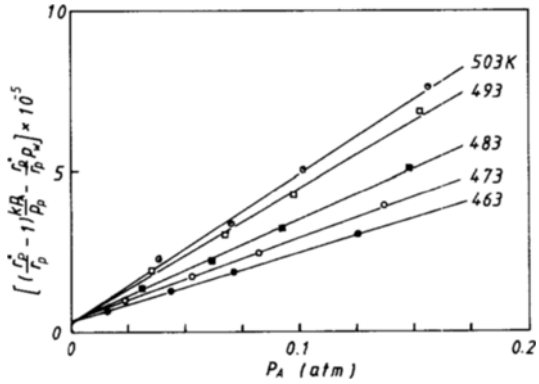

Fig. 10. Relationship between the left-hand side term and IPA pressure in eq. (7).

may conclude that a saturation of the surface with chemisorbed alcohol molecules has been reached under these circumstances. Isopropyl ether, which has been reported to be produced simultaneously with olefins on most oxide catalysts [9,13,14], was not detected. The ether formation was known to be dependent on the stability of the surface alcoholate species, which does decrease with chain length and branching in alcohols [14]. Therefore, it appeares likely that the surface alcoholate species in the circumstances explored is unstable because of its branch and higher reaction temperature.

We may expect that propene desorbs immediately and doesn't interfere with the reaction rates. However, water is also produced, and we may expect water molecules to stay adsorbed or become adsorbed immediately after the reaction. Really, it is known from the literatures [9,16,18] that water is a strong inhibitor of these reactions and the strength of adsorption of water is higher than that of alcohol. Also there are many evidences for reversible IPA adsorption [16, 17]. Taking into account all these findings, the suggested chemical sequence for dehydration seems to be very reasonable. To check the agreement of the derived rate eq. (5), a plot

Table 4. Activation energies for IPA decomposition on various metal oxides.

catalyst	surface area (m^2/g-cat)	dehydration activation energy (Kcal/mole)	dehydrogenation activation energy (kcal/mole)	reference
Mo-Al_2O_3 a	200	22.8	13.2	this work
Al_2O_3 [b]	–	31	–*	(19)
Al_2O_3 [d]	100	31	33.7	(19)
SiO_2 [c]	587	23	–*	(19)
TiO_2 (rutile)	5.5	34	18	(19)
TiO_2 (anatase)	170	35.5	26	(19)
TiO_2 [e]	50	34	15	(19)
V_2O_5 [c]	2.6	20	14	(19)
MnO_2 [c]	26.7	24	11	(19)
γ-Al_2O_3	230	32	–	(20)
Thoria	55	29.5	–	(20)
Silica-Alumina [f]	700	30	–	(20)
Cr_2O_3	–	–	13±1**	(21)
$ZnCr_2O_4$	–	–	8±1**	(21)
γ-Al_2O_3 [g]	–	27.3±0.4	–	(18)

a, oxidizing cat. (7.6% Mo) b, 99.999% c, sorbosil d, Degussa-type C e, Degussa-type P25
f, Ketjen (13% Al_2O_3) g, Degussa-type P110 C 1
* no activity for dehydrogenation ** calaulated from Arrhenius plot

of $\{(\frac{r_p^o}{r_p}-1)\frac{K P_A}{P_p}-\frac{r_p^o}{r_p}P_W\}$ versus P_A at constant temperature was made, which should be linear with positive slope and intercept if the mechanism associated with eq. (5) is correct. This plot is shown in Fig. 10 and the lines are essentially straight as predicted.

In Table 4, the activation energies are given. In spite of different catalysts, the activation energy in this work agrees fairly with those [18, 19] measured in a dynamic reactor. It is also found that the activation energy for molybdena-alumina employed in this work is lower than those [18, 19] for pure alumina generally. This may have some relations with the change of catalyst acidity due to Mo loading; many investigators [22-24] reported that no Brønsted acid site (only Lewis acid site) was found on the parent alumina surface even in the presence of H_2O. But, on oxidized molybdena-alumina catalyst, the Brønsted acidity was discovered to be formed newly whereas the Lewis acidity falled [23, 24].

Bremer and coworkers [25, 26] thought that the moleculary adsorbed alcohol was hydrogen-bonded to Brønsted acid sites and not to Lewis acid ones, which was later confirmed by IR study [27]. In contrast to molecular adsorption, others [9, 28, 29] believe that the alcohol is dissociatively adsorbed on Lewis acid sites to form a surface alkoxide and an adsorbed proton. Taking into account these different mechanisms, some conclusion can be made. i.e., alcohol adsorbs dissociatively on Lewis center and, on Brønsted one does occur a molecular adsorption whose heat of adsorption may be higher than the former. If all these two sites are present, two type adsorption occur simultaneously. Therefore, it is reasonable that the activation energy for the unreduced Mo-Al_2O_3 catalyst, on which Brønsted and Lewis centers coexist, is lower than that for pure alumina.

In preliminary experiments, it was found that the parent alumina had no activity for dehydrogenation of IPA. But, on the oxidized Mo-Al_2O_3, does occur the dehydrogenation reaction. It is easily explained in terms of the Krylov's simple arguments [30]. According to his arguments, strong metal-oxygen bond (M-O) gives strong acidity and, in oxides that have weak M-O bonds, the oxygen lone pair is basic and binds strongly to acidic molecules. In this regard, Al_2O_3 is very acidic and MoO_3 is slightly acidic [30]. Therefore the dependence of dehydrogenation activity on Mo loading is likely due to the development of O^{-2} on MoO_3, giving base sites which is essential in the concerted mechanism proposed by many investigators [3, 5, 6].

In view of simplifications involved in the derived rate equations (6), the consistency is rather satisfactory; the similar rate expression with ours was found suitable also by Garcia De La Banda [21] and L. Nondek [31] for the dehydrogenation of secondary alcohols on a ZnO-Cr_2O_3 and on a Cr_2O_3 catalyst, respectively.

The value of activation energy for dehydrogenation shows a good agreement with others [19, 21]. An interesting aspect is that the adsorption enthalpies of IPA for two reactions, dehydration and dehydrogenation, are different each other. Although this result seems to be in conflict, it is rather consistent with our assumption which dehydration and dehydrogenation take place independently.

Dependence of acid-base property on reduction

The values of r_p and r_k/r_p for various treatments of catalyst are listed in Table 3. As previously discussed, r_p represents the rough trend for acidity and r_k/r_p does for basicity. In this regard, acidity and basicity on the Mo-Al_2O_3 was found to be affected by the extent of reduction; the acidity decreases rapidly during the initial stage of reduction. As the catalyst is further reduced, the acidity increases gradually, and for basicity vice versa.

In order to correlate the data obtained by Hall's IR research [23], another separate experiment in which the same reduction conditions such as theirs [23] were employed was carried out. These results show a relatively good agreement with total acidity, $B_{py}+L_{py}$, which was found to increase as the catalyst was reduced further (Fig. 11). More recently, Suarez [24] reported the different data that total acidity increase to a maximum and then to decrease as the catalyst is reduced further; but

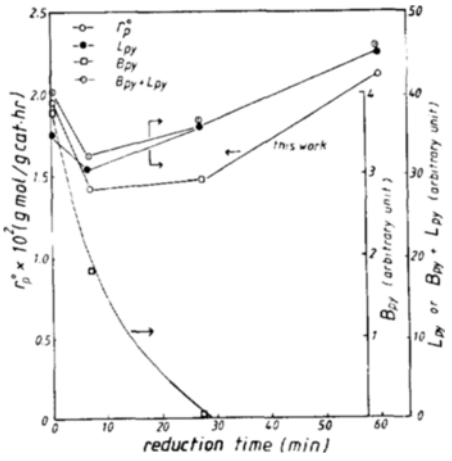

Fig. 11. Correlation of initial rate of dehydration with the Hall's data (23); H_2 flow rate (reduction) = 100ml (NTP)/min., reaction temperature = 503K, B_{py} represents the amount of pyridine adsorbed on the Bronsted acid sites, L_{py} is for pyridine adsorbed in Lewis acid sites.

weaker Lewis acidity ($L_{py}(I)$) itself represents the reverse trend (Table 3).

Correlating these results with ours, it is not conclusive, but appears likely that the active centers for dehydration are Brønsted acid site and weaker Lewis acid site on the Mo-Al_2O_3 catalyst.

We suggest that the above findings can be explained in terms of surface chemistry on molybdena-alumina. The surface of the raw catalyst after oxidizing with oxygen above 720 K contains patches of a polymolybdate species [32]. These small clusters of 7 or so Mo atoms with their associated oxygen become bound to the surface on calcination. Upon reduction, some of these surface bonds are broken as missing alumina hydroxyl groups are reformed, thereby producing Brønsted acid sites. These reformed Brønsted sites disappear due to the decrease of electronegativity as the catalyst is further reduced, which has been confirmed by IR investigation [23,24].

Lewis acidity seems to be responsible for the area of the uncovered portions of the alumina surface; the decrease of Lewis acidity during the initial stage of the reduction may be due to the new hydroxyl groups on the Lewis acid ones. It is evident from the findings of Hall and his coworkers [33] that up to half the consumed hydrogen remained on the catalyst as new hydroxyl groups during the early stages of the reduction. The details of this Lewis acidic property are discussed elsewhere [24]. In contrast to acidity, few evidences for basicity have been represented. Hall and his coworkers [34] found that NO is a selective poison for propene hydrogenation which may be related to basicity. In related IR experiment [35], NO was found to be adsorbed only on the coordinately unsaturated sites (CUS) of the reduced molybdena surface. From these findings, it can be deduced that the CUS associated to molybdena plays a role of basic site. This consideration, however, is not yet clear. The dilemma presented suggests a promising area for further research.

ACKNOWLEDGEMENT

One of the authors, K.T. Seo wishes to acknowledge the financial support by Korea Science and Engineering Foundation for this study.

NOMENCLATURE

A	: gaseous reactant, isopropyl alcohol	
E	: activation energy	(kcal/g-mol)
F_A°	: feed rate of isopropyl alcohol	(g-mol/hr)
k	: reaction rate constant for propene-formation	(g-mol/g-cat hr)
k'	: constant in eq. (3)	(g-mol/g-cat)
k_k	: constant in eq. (2)	(g-cat/g-mol hr)
k_p	: constant in eq. (1)	(1/hr)
k_{sr}	: reaction rate constant for acetone-formation	(g-mol/g-cat hr)
K	: thermodynamic equilibrium constant	(atm)
K_A, K_A'	: adsorption equilibrium constant of isopropyl alcohol	(1/atm)
K_p	: adsorption equilibrium constant of propene	(1 atm)
K_W	: adsorption equilibrium constant of water	(1/atm)
LHSV	: liquid hourly space velocity	(g-cat hr/g-mol)
P	: gaseous reaction product, propene	
P_A°	: initial pressure of isopropyl alcohol	(atm)
P_A	: partial pressure of isopropyl alcohol	(atm)
P_P	: partial pressure of propene	(atm)
P_W	: partial pressure of water	(atm)
Q_A	: heat of adsorption of isopropyl alcohol for propene formation	(kcal/g-mol)
Q_A'	: heat of adsorption of isopropyle alcohol for acetone formation	(kcal/g-mol)
Q_W	: heat of adsorption of water for propene formation	(kcal/g-mol)
r_k	: reaction rate of acetone formation	(g-mol/g-cat hr)
r_p	: reaction rate of propene formation	(g-mol/g-cat hr)
r_p°	: initial reaction rate of propene formation	(g-mol/g-cat hr)
x	: total conversion of isopropyl alcohol	(—)
x_k	: conversion to acetone	(—)
x_p	: conversion to propene	(—)
W	: gaseous reaction product, water	
W	: mass of catalyst	(g-cat)

REFERENCES

1. Massoth, F.E.: "Advances in Catalysis", vol. 27, p. 265, Academic press, New York, NY (1978).
2. Ai, M. and Suzuki, S.: *J. Catal.*, **30,** 362 (1973).
3. Ai, M.: *Bull. Jap. Petrol. Inst.*, **18,** 50 (1976).
4. Ai, M.: *Bull. Chem. Soc. Jap.*, **49,** 1328 (1976).
5. Ai, M.: *Bull. Chem. Soc. Jap.*, **50,** 355 (1977).
6. Ai, M.: *Bull. Chem. Soc. Jap.*, **50,** 2579 (1977).
7. Tanabe, K.: "Catalysis Science and Technology" vol. 2, p.231, Springer-Verlag, Berlin (1981).
8. Pines, H.: *Adv. Catal.*, **16,** 49 (1966).
9. Soma, Y., Onishi, T. and Tamaru, K.: *Trans, Faraday Soc.*, **65,** 2215 (1969).

10. Wang, L. and Hall, W.K.: *J. Catal.*, **77,** 232 (1982).
11. Yang, K.H. and Hougen, O.A.: *Chem. Eng. Prog.*, **46,** 146 (1950).
12. Kittrell, J.R. and Mezaki, R.: *A.I. Ch. E.J.*, **13,** 389 (1967).
13. De Boer, J.H., et al: *J. Catal.*, **7,** 163 (1967).
14. Knözinger, H., Bühl, H. and Ress, E.: *J. Catal.*, **12,** 121 (1968).
15. Knözinger, H. and Köhne, R.: *J. Catal.*, **5.** 264 (1966).
16. Pepe, F. and Stone, F.S.: *J. Catal.*, **56,** 160 (1979).
17. Kolbe, S.: *J. Catal.*, **13.** 193 (1969).
18. Knözinger, H. and Scheglide, A.: *J. Catal.*, **17,** 252 (1970).
19. Cunningham, J., Hondett, B.K., Ilyes, M., Tobin, J., Leahy, E.L. and Fierro, J.L.G.: *Faraday Disc. Chem. Soc.*, **72,** 283 (1981).
20. De Mourgues, L. and Peyron, F., Trambouze, Y. and Prettre, M.: *J. Catal.*, **7,** 117 (1967).
21. Juan F. Garcia De La Banda: *J. Catal.*, **1,** 136 (1962).
22. Fransen, P.T., Vander Meer, O. and Mars, P.: *J. Phys. Chem.*, **80,** 2103 (1976).
23. Segawa, K. and Hall, W.K.: *J. Catal.*, **76,** 133 (1982).
24. Suarez, W.: M.S. Thesis, Univ., of Wisconsin-Madison, Madison, U.S.A. (1984).
25. Bremer, H., Steinberg, K.H. Glietsch, J., Lusky, H., Werher, U. and Wendlandt, K.D.: *Z. Chem.*, **10,** 161 (1970).
26. Bremer, H., Steinberg, K.H. and Wendlandt. K.D.: *Z. Anorg. Allge. Chem.*, **366,** 130 (1969).
27. Knözinger, H. and Stoltz, H.: *Ber Bunsen. Phys. Chem.*, **74,** 1056 (1970).
28. Arai, H., Take, J., Saito, Y. and Yoneda, Y.: *J. Catal.*, **9,** 146 (1967).
29. Kagel, R.O.: *J. Chem. Phys.*, **71,** 844 (1967).
30. Krylov., O.V.: "Catalysis by Non-metals", P. 70, Academic Press, New York, NY (1970).
31. Nondek, L. and Kraus, M.: *J. Catal.*, **40,** 40 (1975).
32. Wang, L. and Hall, W.K.: *J. Catal.*, **66,** 251 (1980).
33. Hall, W.K. and Massoth, F.E.: *J. Catal.*, **34,** 41 (1974).
34. Lombardo, E.A., Lojacono, M. and Hall, W.K.: *J. Catal.*, **64,** 150 (1980).
35. Segawa, K. and Hall, W.K.: *J. Catal.*, **77,** 221 (1982).